J. Phys. B: At. Mol. Opt. Phys. **31** (1998) 49–63. Printed in the UK PII: S0953-4075(98)86707-2

Hydrogen atom moving across a strong magnetic field: analytical approximations

A Y Potekhin†

Ioffe Physico-Technical Institute, Politekhnicheskaya 26, St Petersburg 194021, Russia

Received 8 August 1997

Abstract. Analytical approximations are constructed for binding energies, quantum-mechanical sizes and oscillator strengths of main radiative transitions of hydrogen atoms arbitrarily moving in magnetic fields $\sim 10^{12}$–10^{13} G. Examples of using the obtained approximations for determination of maximum transverse velocity of an atom and for the evaluation of absorption spectra in magnetic neutron-star atmospheres are presented.

1. Introduction

An atom moving across a magnetic field is equivalent to an atom placed in perpendicular magnetic and electric fields. We consider the hydrogen atom moving in a magnetic field $\boldsymbol{B}$, strong enough to significantly squeeze the electron wavefunction. Quantitatively, the parameter $\gamma = \hbar\omega_c/(2\ \mathrm{Ryd}) = B/(2.35 \times 10^9\ \mathrm{G})$ is assumed large. Here, $\omega_c = eB/m_e c$ is the electron cyclotron frequency and $\mathrm{Ryd} = m_e e^4/2\hbar^2$ is the ground-state energy of the field-free atom.

Although only small values of γ are available in the laboratory, large values are not uncommon in astrophysics. Spectra of some white-dwarf stars have been interpreted as produced by hydrogen at field strengths between 10^6 and 10^9 G (Wunner and Ruder 1987, Fassbinder and Schweizer 1996, and references therein). Neutron stars which are observed as radio pulsars reveal field strengths in excess of 2×10^8 G, and over half of them possess magnetic fields from 10^{12} to 2×10^{13} G (Taylor *et al* 1993). Absorption of radiation by strongly magnetized atomic hydrogen may have large effects on ultraviolet and x-ray spectra of the neutron stars, which are measured with modern space telescopes (Pavlov *et al* 1995).

The physics of solid state presents another important field of application of quantum-mechanical calculations of strongly magnetized hydrogen atoms. Excitons and shallow impurities in semiconductors reveal hydrogen-like spectra with scaled values of ω_c and Ryd. Such scaling offers a possibility to reach the regime $\gamma > 1$ in an experiment (e.g. Elliott and Loudon 1960, Klaassen *et al* 1997).

The non-moving hydrogen atom in a strong magnetic field was thoroughly studied in the past two decades (Ruder *et al* 1994, and references therein). Extensive tables of binding energies have been presented by Rösner *et al* (1984) and supplemented by Wintgen and Friedrich (1986), Ivanov (1988), Xi *et al* (1992) and Kravchenko *et al* (1996). Tables of oscillator strengths at various values of γ have been published by Forster *et al* (1984); analytical fits to photoionization cross sections at $\gamma \gg 1$ have been proposed by Potekhin and Pavlov (1993).

† E-mail address: palex@astro.ioffe.ru

0953-4075/98/010049+15$19.50 © 1998 IOP Publishing Ltd

The problem of a moving atom (or an atom in crossed fields) is much more complicated because of the absence of axial symmetry. Much work has been done at low field strengths (e.g. Melezhik 1993), where the second-order perturbation theory was applicable (e.g. Braun and Solov'ev 1984, and references therein). The simplifying approximation of infinite proton mass, exploited in this regime, breaks down in strong fields because of collective motion effects studied in detail by Avron *et al* (1978), Baye and Vincke (1990) and Dippel *et al* (1994). In particular, so-called decentred states (with the electron localized mostly in the 'magnetic well' aside from the Coulomb centre) are likely to be populated. These exotic states have been predicted by Burkova *et al* (1976) and studied by Ipatova *et al* (1984), Baye *et al* (1992), Dzyaloshinskii (1992) and Schmelcher (1993). As well as the usual 'centred' states, the decentred states have an infinite discrete energy spectrum (Potekhin 1994, hereafter paper I). Collective-motion effects on the centred states of the strongly magnetized hydrogen atom have been considered by Vincke and Baye (1988) and Pavlov and Mészáros (1993) in frames of the theory of perturbation.

Completely non-perturbative results, covering both centred and decentred states as well as the transition region, were first presented by Vincke *et al* (1992) for binding energies and wavefunctions. In paper I, additionally, oscillator strengths have been considered. Pavlov and Potekhin (1995), hereafter paper II, studied spectral line shapes, and Potekhin and Pavlov (1997) calculated photoionization cross sections. None of these numerical results, however, has been published in an easy-to-use form of tables or analytical expressions. This paper provides such expressions for the magnetic field strengths typical of neutron stars, $300 \leqslant \gamma \leqslant 10^4$. This range is physically distinguished, since at weaker fields the transition region is strongly complicated by multiple narrow anticrossings (Vincke *et al* 1992). The relative simplicity of the spectrum at $\gamma \gtrsim 300$ facilitates analytical description. The upper bound, $\gamma \sim 10^4$, corresponds to the onset of non-negligible relativistic effects (Chen and Goldman 1992).

In the next section we recall the basic definitions and physical properties of a hydrogen atom arbitrarily moving in a strong magnetic field. In section 3, we first present accurate analytical fits to binding energies, depending on the state of motion, for a number of bound states and various field strengths. Then we derive analytical approximations continuously depending on γ. As a by-product, simple and accurate approximations are obtained for binding energies of the non-moving atom at any $\gamma \gtrsim 1$. The obtained formulae are applied to evaluation of the maximum transverse velocity of the strongly magnetized atom. Section 4 is devoted to analytical approximations of quantum-mechanical sizes and main oscillator strengths of the atom. In section 5, an example of using the obtained expressions for calculation of absorption coefficients of strongly magnetized, hot hydrogen plasma is presented.

2. Centred and decentred states: general description

Motion of the hydrogen atom in a magnetic field can be conveniently described by the pseudomomentum (e.g. Johnson *et al* 1983)

$$\boldsymbol{K} = m_{\rm p}\dot{\boldsymbol{r}}_{\rm p} + m_{\rm e}\dot{\boldsymbol{r}}_{\rm e} - \frac{e}{c}\boldsymbol{B} \times (\boldsymbol{r}_{\rm e} - \boldsymbol{r}_{\rm p}), \tag{1}$$

where the subscript $i = {\rm e}$ or $i = {\rm p}$ indicates electron or proton, respectively,

$$\dot{\boldsymbol{r}}_i = \frac{\rm i}{\hbar}[H_{\rm tot}, \boldsymbol{r}_i] = -\frac{{\rm i}\hbar}{m_i}\nabla_i - \frac{q_i}{m_i c}\boldsymbol{A}(\boldsymbol{r}_i) \tag{2}$$

is the velocity operator, m_i the mass, $q_p = -q_e = e$ the charge, $\boldsymbol{A}(\boldsymbol{r})$ the vector potential of the field, and H_{tot} the two-particle Hamiltonian operator. Gorkov and Dzyaloshinskii (1968) have shown that in the representation in which all three components of $\boldsymbol{K}$ have definite values the pseudoseparation of the centre-of-mass motion can be performed, that is, the relative motion can be described in terms of a one-particle Hamiltonian which depends on $\boldsymbol{K}$. The expectation value of the velocity of the atom is $\nabla_{\boldsymbol{K}} E$, where E is the expectation value of the energy.

It is convenient to describe the centred states of the atom using the relative coordinate $\boldsymbol{r}^{(0)} = \boldsymbol{r}_e - \boldsymbol{r}_p$ as independent variable and the axial gauge of the vector potential, $\boldsymbol{A}(\boldsymbol{r}) = \frac{1}{2}\boldsymbol{B} \times \boldsymbol{r}$. For the decentred states, the 'shifted' representation (Gorkov and Dzyaloshinskii 1968) is more convenient. In the latter representation, the independent variable is $\boldsymbol{r}^{(1)} = \boldsymbol{r}_e - \boldsymbol{r}_p - \boldsymbol{r}_c$ and the gauge is $\boldsymbol{A}(\boldsymbol{r}) = \frac{1}{2}\boldsymbol{B} \times (\boldsymbol{r} - [(m_p - m_e)/m_H]\boldsymbol{r}_c)$. Here, $\boldsymbol{r}_c = (c/eB^2)\boldsymbol{B} \times \boldsymbol{K}$ is the relative guiding centre and $m_H = m_p + m_e$ is the mass of the atom.

Let us assume that $\boldsymbol{B}$ is directed along the z-axis. The z-component of the pseudomomentum corresponding to the motion along the field separates exactly from the Hamiltonian, giving the kinetic term $K_z^2/2m_H$, while the transverse components $\boldsymbol{K}_\perp$ produce non-trivial effects. Therefore we assume $K_z = 0$ and $\boldsymbol{K}_\perp = \boldsymbol{K}$ hereafter.

If there were no Coulomb attraction, then the electron Landau number $n = 0, 1, 2, \ldots$ and the z-projection s of the angular momentum of the relative motion would be exact quantum numbers (since $\boldsymbol{K}$ is definite, the electron and proton do not possess definite z-projections of the angular momenta separately from each other—see Johnson *et al* 1983). In this case the transverse part of the wavefunction could be described by a Landau function $\Phi_{ns}(\boldsymbol{r}_\perp^{(1)})$, where $\boldsymbol{r}_\perp^{(1)}$ is the projection of $\boldsymbol{r}^{(1)}$ in the (xy)-plane and s is defined in the shifted reference frame (e.g. paper I). The energy of the transverse excitation (with the zero-point and spin terms subtracted) is

$$E_{ns}^{\perp} = [n + (m_e/m_p)(n + s)]\hbar\omega_c. \tag{3}$$

A wavefunction ψ_κ of an atomic state $|\kappa\rangle$ can be expanded over the complete set of the Landau functions

$$\psi_\kappa^{(\eta)}(\boldsymbol{r}^{(\eta)}) = \sum_{ns} \Phi_{ns}(\boldsymbol{r}_\perp^{(\eta)}) g_{n,s;\kappa}^{(\eta)}(z), \tag{4}$$

where $\eta = 0$ or 1 indicates the conventional or shifted representation, respectively (a generalization to continuous η in paper I proved to be less useful). The adiabatic approximation used in early works (Gorkov and Dzyaloshinskii 1968, Burkova *et al* 1976) corresponds to retaining only one term in this expansion.

A bound state can be numbered as $|\kappa\rangle = |ns\nu\boldsymbol{K}\rangle$, where n and s relate to the leading term of the expansion (4), and ν enumerates longitudinal energy levels

$$E_{ns\nu}^{\parallel}(K) = E_\kappa - E_{ns}^{\perp} \tag{5}$$

and controls the z-parity: $g_{n,s;\kappa}^{(\eta)}(-z) = (-1)^\nu g_{n,s;\kappa}^{(\eta)}(z)$. This way of numbering is conventional for the non-moving atom at $\gamma \gtrsim 1$. The states $\nu = 0$ are tightly bound in the Coulomb well, while the states $\nu \geqslant 1$ are hydrogen-like, with binding energies below 1 Ryd. For a moving atom, this way of numbering remains unambiguous at $\gamma \gtrsim 300$, in spite of the fact that there may not exist an obvious leading term of (4) in this case (paper I).

The inequality $E_\kappa < 0$ determines truly bound states, as opposed to the ones subject to autoionization. In particular, all states with $n \neq 0$ belong to continuum at $\gamma \gtrsim 0.2$ and will not be considered hereafter.

Since the transverse factors Φ_{ns} in (4) are known analytically, only the one-dimensional longitudinal functions $g^{(\eta)}_{ns;\kappa}$ are to be found numerically. An algorithm which is most efficient at $\gamma \gg 1$ has been described in paper I. At small pseudomomenta K, the states $\nu = 0$ remain tightly bound and centred, the average electron–proton displacement $\bar{x}$ being considerably smaller than r_c. For the hydrogen-like states $\nu \geqslant 1$, however, $\bar{x}$ is close to r_c at any K.

According to the second-order perturbation approximation at small K, the absolute expectation value of the velocity $v = \partial E_\kappa / \partial K$ in a bound state $|\kappa\rangle$ equals $K/M^{\perp}_{ns\nu}$, where $M^{\perp}_{ns\nu}$ is the effective 'transverse' mass (Vincke and Baye 1988, Pavlov and Mészáros 1993). $M^{\perp}_{ns\nu}$ always exceeds m_H, and it is greater the stronger the field and the higher the considered atomic level.

The larger K, the greater is the distortion of the wavefunction towards $\boldsymbol{r}_c$, caused by the motion-induced electric field in the co-moving reference frame. The perturbation approximation becomes increasingly inaccurate, until near some critical value K_c a transition to the decentred state occurs, and the character of the motion totally changes. With further increasing K, the transverse velocity decreases and tends to zero, while the electron–proton separation increases and tends to r_c. Thus, for the decentred states, the pseudomomentum characterizes electron–proton separation rather than velocity.

The shifted ($\eta = 1$) adiabatic approximation becomes fairly good at $K \gg K_c$. At very large K the longitudinal functions become oscillator-like, corresponding to a wide, shallow parabolic potential well of a depth $\simeq e^2/r_c$ (Burkova *et al* 1976). For a fixed ν, this limit is reached at $K \gg (\nu + \frac{1}{2})^2 \hbar / a_B$, where a_B is the Bohr radius. Still at arbitrarily large K there remain an infinite number of bound states with high values of ν whose longitudinal wavefunctions are goverened by the Coulomb tail rather than by the parabolic core of the effective one-dimentional potential (paper I).

The decentred states of the atom at $K > K_c \sim 10^2$ au have relatively low binding energies and large quantum-mechanical sizes, $l \sim K/\gamma$ au; therefore they are expected to be destroyed by collisions with surrounding particles in the laboratory and in the white-dwarf atmospheres. In neutron-star atmospheres at $\gamma \gtrsim 10^3$, however, the decentred states may be significantly populated (paper II). This necessitates inclusion of the entire range of K below and above K_c in the consideration.

3. Binding energies

3.1. Dependence of the energies on the pseudomomentum at selected field strengths

We have calculated binding energies of the hydrogen atom moving across the strong magnetic field at $\gamma = 300$, 600, 1000, 2000, 3000 and 10 000 for several lowest tightly bound and hydrogen-like states, using the technique described in paper I. At each value of γ and for each state, the calculations have been performed at $K = 0$ and at about 50–100 values of K from $K \leqslant 10$ to $K \geqslant 10^4$ au, approximately equidistant in $\log K$ but with additional points near avoided crossings. The calculated energies have an accuracy of 3–5 digits.

In applications, however, one usually has to deal with a distribution of atoms over a more or less broad band of values of the pseudomomentum K and calculate the observable quantities by averaging over K. This makes it highly desirable to have an analytical approximation of the K-dependence of the energies, $E(K)$. Lai and Salpeter (1995) were the first to present an analytical fit to $E(K)$, which was rather accurate for the ground state at $K < K_c$ but could not be applied to excited or decentred states.

We describe the longitudinal energy (5) by the formula

$$|E^{\parallel}_{n s \nu}(K)| = \frac{E^{(1)}_{n s \nu}(K)}{1 + (K/K_{\rm c})^{1/\alpha}} + \frac{E^{(2)}_{n s \nu}(K)}{1 + (K_{\rm c}/K)^{1/\alpha}}. \tag{6}$$

The two-term structure of (6) is dictated by the necessity to describe the two physically distinct regions of K below and above $K_{\rm c}$. The parameter α has the meaning of the width of the transition region near $K_{\rm c}$ in logarithmic scale of pseudomomenta. As noted in paper I, for the tightly bound states $K_{\rm c}$ is close to $(2m_{\rm H}E^{(0)}_{n s \nu})^{1/2}$, where $E^{(0)}_{n s \nu} \equiv -E^{\parallel}_{n s \nu}(0)$. We write $K_{\rm c} = q_0(2m_{\rm H}E^{(0)}_{n s \nu})^{1/2}$ and treat q_0 as a fitting parameter.

Intricate structure of the region of avoided crossings (see Vincke *et al* 1992) complicates its accurate analytical description. We have chosen to keep our formulae simple at the cost of decreasing accuracy near these crossings.

For the tightly bound states, we parametrize the functions $E^{(j)}(K)$ as follows:

$$E^{(1)}_{0s0}(K) = E^{(0)}_{0s0} - \frac{K^2}{2m_{\rm eff} + q_1 K^2/E^{(0)}_{0s0}}, \tag{7}$$

$$E^{(2)}_{0s0}(K) = 2[r_*^2 + r_*^{3/2} + q_2 r_*]^{-1/2}\ \text{Ryd}, \tag{8}$$

where $r_* = r_{\rm c}/a_{\rm B} = K/(\gamma\ \text{au})$, q_1 and q_2 are dimensionless fitting parameters, and $m_{\rm eff}$ is the effective mass which is close to (but not necessarily coincident with) the transverse effective mass $M^{\perp}_{n s \nu}$ obtained by the perturbation technique.

In the considered range of γ, the parameter q_1 can be approximated as

$$q_1 = \begin{cases} \lg(\gamma/300) & \text{if } s = 0, \\ 0.5 & \text{otherwise.} \end{cases}$$

Optimal values of the other parameters are listed in table 1. The last column presents the root-mean-square (rms) difference σ_E between the computed and fitted energies. Maxmum errors of the fit ($\lesssim 3\sigma_E$) occur near the avoided crossings.

Binding energies of the hydrogen-like states are approximated by the same formula (6) but with slightly different expressions for $E^{(1)}$ and $E^{(2)}$. For these states, $M^{\perp}_{n s \nu}$ exceeds $m_{\rm H}$ by orders of magnitude and the perturbation method fails even at small values of K (Pavlov and Mészáros 1993), which renders the notion of transverse mass practically useless for the fitting. Thus we consider $m_{\rm eff}$ as effectively infinite and put $E^{(1)}_{0s\nu} = E^{(0)}_{0s\nu}$ ($\nu \geqslant 1$). Furthermore, the transition region is not well defined, therefore $K_{\rm c}$ and α lose their clear meaning and become mere fitting parameters.

The function $E^{(2)}(K)$ that describes the longitudinal energy at large K is now

$$E^{(2)}_{0s\nu}(K) = \{(2\ \text{Ryd})^{-1}[r_*^2 + (2\nu+1)r_*^{3/2} + q_2 r_*]^{1/2} + 1/E^{(0)}_{0s\nu}\}^{-1}, \tag{9}$$

where r_* and $E^{(0)}$ have the same meaning as before. The first and second terms in the square brackets ensure the correct asymptotic behaviour (paper I). In this case,

$$q_2 = \begin{cases} \nu^2 - 1 & (\text{odd } \nu) \\ \nu^2 + 2^{\nu/2}\lg(\gamma/300) & (\text{even } \nu). \end{cases}$$

Optimal values of the parameters q_0 and α are listed in table 2. As well as in table 1, the last column presents rms errors which are several times smaller than the maximum errors near anticrossings.

In both tables 1 and 2, only truly bound (not autoionizing) states are considered. For example, all states with $s > 0$, $\nu > 0$ belong to continuum at $\gamma > 673$, therefore table 2 does not contain entries for them at $\gamma = 1000$ and higher.

Table 1. Parameters of the analytical approximation (6)–(8) for the energies of tightly bound states $|0s0\rangle$.

s	γ	$E^{(0)}$ (Ryd)	$\lg(m_{\rm eff}/m_{\rm H})$	q_0	α	q_2	σ_E (Ryd)
0	300	10.722	0.009	0.859	0.001	0.102	0.028
	600	13.210	0.042	0.811	0.107	0.157	0.040
	1 000	15.325	0.072	0.823	0.117	0.189	0.025
	2 000	18.610	0.141	0.850	0.178	0.233	0.018
	3 000	20.770	0.175	0.873	0.191	0.244	0.017
	10 000	28.286	0.319	1.019	0.173	0.275	0.027
1	300	7.669	0.161	0.963	0.132	0.115	0.026
	600	9.607	0.269	1.060	0.093	0.160	0.021
	1 000	11.277	0.369	1.147	0.060	0.176	0.024
	2 000	13.904	0.578	1.195	0.122	0.215	0.016
	3 000	15.649	0.701	1.202	0.147	0.235	0.014
	10 000	21.830	0.944	1.337	0.298	0.240	0.033
2	300	6.450	0.304	1.184	0.030	0.120	0.017
	600	8.142	0.497	1.197	0.081	0.181	0.014
	1 000	9.610	0.643	1.262	0.074	0.195	0.014
	2 000	11.937	0.931	1.291	0.127	0.230	0.014
	3 000	13.493	1.093	1.320	0.153	0.240	0.022
3	300	5.734	0.466	1.263	0.039	0.122	0.015
	600	7.274	0.701	1.273	0.082	0.183	0.012
	1 000	8.617	0.897	1.347	0.090	0.204	0.018
	2 000	10.755	1.252	1.403	0.131	0.232	0.019
	3 000	12.191	1.451	1.457	0.154	0.240	0.026
4	300	5.243	0.616	1.330	0.050	0.128	0.013
	600	6.676	0.892	1.342	0.095	0.194	0.011
	1 000	7.929	1.124	1.437	0.096	0.211	0.017
	2 000	9.933	1.555	1.544	0.114	0.229	0.016
5	300	4.877	0.755	1.391	0.058	0.128	0.012
	600	6.227	1.086	1.393	0.107	0.199	0.012
	1 000	7.413	1.354	1.545	0.130	0.229	0.010
6	300	4.589	0.888	1.448	0.062	0.123	0.013
	600	5.874	1.281	1.441	0.121	0.207	0.013
	1 000	7.004	1.668	1.587	0.107	0.210	0.018
7	300	4.355	1.021	1.504	0.070	0.132	0.013
	600	5.585	1.480	1.473	0.139	0.213	0.014

3.2. Two-dimensional approximations

Equations (6)–(9) help us to derive approximations of the binding energies as functions of two continuous arguments γ and K. For this purpose, we replace the numerical parameters listed in tables 1 and 2 by analytical functions of γ.

One of these parameters—the longitudinal energy of the atom at rest $E^{(0)}$—has an independent significance. For this reason, we have constructed an accurate fit to $E^{(0)}$ in the

Table 2. Parameters of the analytical approximation (6) and (9) for the energies of hydrogen-like states $|0s\nu\rangle$, $\nu \geqslant 1$.

s	ν	γ	$E^{(0)}_{0s\nu}$ (Ryd)	q_0	α	σ_E (Ryd)
0	1	300	0.964 3	1.751	0.7081	0.001 3
		600	0.978 1	3.019	0.7441	0.001 3
		1 000	0.985 0	4.595	0.7604	0.001 8
		2 000	0.991 2	8.467	0.7977	0.001 7
		3 000	0.993 6	12.43	0.8095	0.001 2
		10 000	0.997 6	39.65	0.8052	0.002 3
0	2	300	0.552 2	1.064	0.6186	0.000 6
		600	0.575 5	1.463	0.6252	0.000 5
		1 000	0.591 7	1.885	0.6322	0.001 8
		2 000	0.612 5	2.632	0.6255	0.000 7
		3 000	0.624 0	3.143	0.6406	0.003 7
		10 000	0.655 4	4.810	0.6573	0.002 2
0	3	300	0.245 6	5.608	0.8501	0.000 5
		600	0.247 3	10.68	0.8495	0.001 3
		1 000	0.248 2	16.67	0.8617	0.000 3
		2 000	0.248 9	31.35	0.8940	0.000 2
		3 000	0.249 2	45.96	0.8966	0.000 2
		10 000	0.249 8	150.1	0.8956	0.000 3
0	4	300	0.181 4	2.145	0.7140	0.002 5
		600	0.185 8	2.868	0.6699	0.000 3
		1 000	0.188 7	3.566	0.6609	0.000 2
		2 000	0.192 4	4.963	0.6165	0.000 2
		3 000	0.194 5	5.908	0.5970	0.000 3
		10 000	0.199 9	8.965	0.5675	0.000 6
0	5	300	0.109 82	10.05	0.9245	0.000 14
		600	0.110 32	18.58	0.9422	0.000 14
		1 000	0.110 57	29.87	0.9404	0.000 10
		2 000	0.110 79	56.85	0.9630	0.000 09
		3 000	0.110 88	83.66	0.9619	0.000 09
		10 000	0.111 04	273.3	0.9745	0.000 06
0	6	300	0.089 20	2.435	0.8688	0.000 54
		600	0.090 68	4.328	0.7156	0.000 16
		1 000	0.091 67	5.237	0.7205	0.000 18
		2 000	0.092 94	7.419	0.6593	0.000 10
		3 000	0.093 62	8.825	0.6237	0.000 16
		10 000	0.095 42	13.43	0.5906	0.000 26
1	1	300	0.940 7	2.109	0.6794	0.001 0
		600	0.964 0	3.553	0.7029	0.002 4
1	2	300	0.513 8	1.930	0.6417	0.003 8
2	1	300	0.922 3	2.421	0.6553	0.001 4

widest possible range of γ values. For the tightly bound states, we have

$$E^{(0)}_{0s0}(\gamma)/\mathrm{Ryd} = \ln(\exp[(1+s)^{-2}] + p_1[\ln(1+p_2\sqrt{\gamma})]^2) + p_3[\ln(1+p_4\gamma^{p_5})]^2. \qquad (10)$$

The parameters p_1–p_5 depend on s; they are presented in table 3. This fit is accurate to

Table 3. Parameters of the analytical approximation (10) for the energies of tightly bound states $|0s0\rangle$ at $10^{-1} \leqslant \gamma \leqslant 10^4$.

s	p_1	p_2	p_3	p_4	p_5
0	15.55	0.378	2.727	0.3034	0.4380
1	0.5332	2.100	3.277	0.3092	0.3784
2	0.1707	4.150	3.838	0.2945	0.3472
3	0.07924	6.110	4.906	0.2748	0.3157
4	0.04696	7.640	5.787	0.2579	0.2977
5	0.03075	8.642	6.669	0.2431	0.2843
6	0.02142	9.286	7.421	0.2312	0.2750
7	0.01589	9.376	8.087	0.2209	0.2682

Table 4. Parameters of the analytical approximations (11)–(13) for the energies of hydrogen-like states $|00\nu\rangle$ at $1 \leqslant \gamma \leqslant 10^4$.

ν	1	2	3	4	5	6
a_ν	0.785	0.578	0.901	0.631	0.970	0.660
b_ν	1.724	0.765	1.847	0.717	1.866	0.693

within 0.1–1% at $\gamma = 10^{-1}$–10^4 and it also provides the correct limits at $\gamma \to 0$.

For the hydrogen-like states, we use the asymptotic result (Haines and Roberts 1969)

$$E^{(0)}_{ns\nu} = \frac{1\ \mathrm{Ryd}}{(n+\delta)^2}, \qquad \text{where} \quad \begin{cases} n = (\nu+1)/2,\ \delta \sim \gamma^{-1} & (\text{odd } \nu) \\ n = \nu/2,\ \delta \sim (\ln\gamma)^{-1} & (\text{even } \nu). \end{cases} \tag{11}$$

We have obtained the following fits to the quantum defect δ: for odd ν,

$$\delta(\gamma) = (a_\nu + b_\nu\sqrt{\gamma} + 0.077\gamma)^{-1}, \tag{12}$$

where $a_\nu \approx 1$ and $b_\nu \approx 2$; and for even ν,

$$\delta(\gamma) = [a_\nu + 1.28\ln(1 + b_\nu\gamma^{1/3})]^{-1}, \tag{13}$$

where $a_\nu \approx \frac{2}{3}$ and $b_\nu \approx \frac{2}{3}$. Accurate values of a_ν and b_ν are given in table 4. At $1 \leqslant \gamma \leqslant 10^4$, rms errors of (12) lie within 3×10^{-4}, and those of (13) within 10^{-3}.

The parameters m_{eff}, α and q_0 in (6)–(9) that determine K-dependences of the energies can also be replaced by analytical functions of γ. Let us start with the tightly bound states ($\nu = 0$). For the effective mass, we have

$$m_{\mathrm{eff}}(\gamma) = m_{\mathrm{H}}[1 + (\gamma/\gamma_0)^{c_0}], \tag{14}$$

where the power index c_0 and the value γ_0 (roughly corresponding to the onset of strong coupling between internal and centre-of-mass motions of the centred atom) depend on the quantum number s and are given by

$$c_0 = 0.937 + 0.038s^{1.58} \qquad \text{and} \qquad \gamma_0 = 6150(1 + 0.0389s^{3/2})[1 + 7.87s^{3/2}]^{-1}.$$

For the critical pseudomomentum, we write

$$q_0 \equiv K_{\mathrm{c}}/\sqrt{2m_{\mathrm{H}}E^{(0)}} = c_1 + \ln(1 + \gamma/\gamma_1). \tag{15}$$

The parameters c_1 and γ_1 take on the values $c_1 = 0.81, 1.09, 1.18, 1.24$ and $\gamma_1 = (8.0, 3.25, 2.22, 1.25) \times 10^4$ for $s = 0, 1, 2, 3$, respectively. For $s \geqslant 4$, we put $c_1 =$

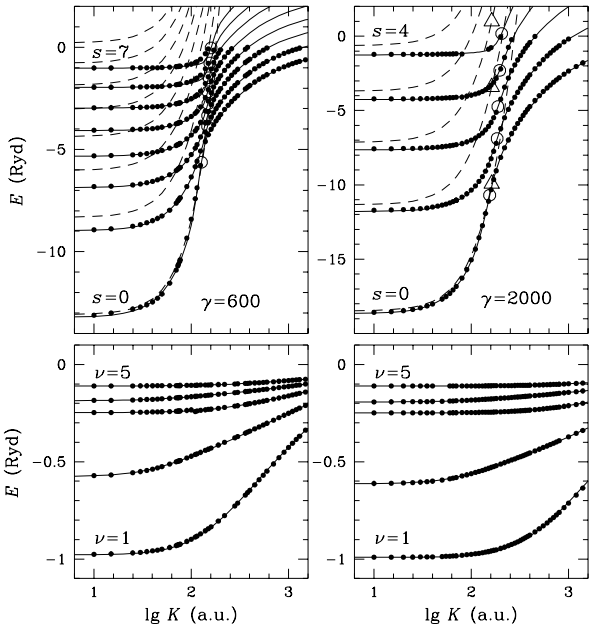

Figure 1. Energy spectrum of the hydrogen atom moving across a strong magnetic field. Upper panels: tightly-bound states ($\nu = 0$); lower panels: hydrogen-like states of the manifold $s = 0$. Numerical values (●) are compared with the analytical approximations of section 3.2 (——) and of Lai and Salpeter (1995) (– – –, upper panels). Triangles (△) mark the limit of validity of the perturbation formalism according to equation (3.8) of Lai and Salpeter; large circles (○) point the present analytical approximation for the critical pseudomomentum K_c.

$0.93 + 0.08s$ and $\gamma_1 = 6500$. The remaining parameters can be replaced by simple expressions, $\alpha = 0.053\ln(\gamma/150)$ and $q_2 = 0.158[\ln((1 + 0.1s)\gamma/215)]^{2/5}$.

Now let us turn to the hydrogen-like states. For odd states, we have, approximately, $q_0 = (\nu^{5/4}\gamma/170)^{0.9}$ and $\alpha = 0.66 + \nu/20$, whereas for even hydrogen-like states $q_0 = \nu\sqrt{\gamma/1200}$ and $\alpha = 0.66$.

These approximations are not so accurate as those provided by tables 1 and 2, but their advantage is that they may be used at arbitrary γ in the range considered. In figure 1 they are compared with our numerical results and with the fitting formulae of Lai and Salpeter (1995). The figure demonstrates that these approximations are valid at any K from 0 to infinity. Noticeable discrepancies between our fitted and calculated data occur only in narrow ranges of K near anticrossings.

3.3. The largest transverse velocity

As an example of application of the above formulae for binding energies, let us estimate the maximum velocity of the atom, $v_{\max} = \max|\partial E/\partial K|$. It can be alternatively interpreted as the maximum transverse electric field $\mathcal{E}_{\rm mov} = v_{\max}B/c$ that could be applied to an atom at rest. A stronger electric field $\mathcal{E} > \mathcal{E}_{\rm mov}$ forces the atoms to move with velocities around the drift velocity of free charges in crossed fields, $\boldsymbol{v}_{\rm drift} = c\boldsymbol{\mathcal{E}} \times \boldsymbol{B}/B^2$, provided that $\mathcal{E} < \mathcal{E}_c = B = 137.036\gamma$ au (in conventional units, $\mathcal{E}_c = 2.998 \times 10^4[B/\mathrm{G}]$ V m^{-1}). Still higher electric field, $\mathcal{E} > \mathcal{E}_c$, cannot be counterbalanced by motion, hence it causes Stark ionization.

Table 5. The largest transverse velocities (in au) in the lowest states $|0s0\rangle$: numerical values $v_{\max}$ compared with the present analytical approximation $v_{\max,\mathrm{appr}}$ and with the approximation $v_{\max,\mathrm{LS}}$ of Lai and Salpeter (1995).

s	0	0	0	0	1	2	3
γ	300	1000	3000	10 000	3000	3000	3000
$v_{\max}$	0.0588	0.0479	0.0372	0.0253	0.0240	0.0198	0.0173
$v_{\max,\mathrm{appr}}$	0.0622	0.0467	0.0367	0.0279	0.0232	0.0187	0.0154
$v_{\max,\mathrm{LS}}$	0.0850	0.0637	0.0548	0.0585	0.0520	0.0571	0.0628

A numerical evaluation of $v_{\max}$ requires multiple calculation of derivatives $\partial E_\kappa/\partial K$ in the most complicated region $K \sim K_\mathrm{c}$. Thus the analytical approximations can be most helpful here. A reasonable approximation is simply $v_{\max,\mathrm{appr}} = \partial|E|/\partial K$ at $K = K_\mathrm{c}$, where E is given by (6) and K_c by (15). Table 5 presents $v_{\max,\mathrm{appr}}$ obtained using this approximation for the lowest tightly bound states along with $v_{\max,\mathrm{LS}}$ given by equation (3.30) of Lai and Salpeter (1995) and with $v_{\max}$ evaluated numerically. The values listed in table (in atomic units of velocity, 1 au = 2188 km s^{-1}) can be translated into those of the critical electric field, $\mathcal{E}_{\mathrm{mov}} = \gamma v_{\max}[\mathrm{au}] \times (5.14 \times 10^{11}$ V m^{-1}).

4. Geometrical characteristics and radiative transitions

4.1. Atomic sizes and dipole moments

Geometrical characteristics of an atom play an important role in distribution of atoms over quantum states in a plasma and in their contribution to the plasma absorption coefficients, since a 'size' of an atom may be used to approximately evaluate effects of destruction of atoms caused by random charge distribution in the plasma (e.g. Potekhin 1996). The K-dependence of rms sizes is complicated and can be non-monotonous near anticrossings. However, the sizes usually need not be known with high precision, that relieves the problem of fitting. The accuracy level of the approximations presented in this section is typically several percent.

At $K = 0$, the atom is axially symmetric, and its rms sizes along the Cartesian coordinates can be approximated as $l_{x0} = l_{y0} \approx a_\mathrm{B}\sqrt{(s+1)/\gamma}$ and

$$l_{z0} \approx \{1/\sqrt{2} + 1/\ln[\gamma/(1+s)]\}(\mathrm{Ryd}/E^{(0)})^{1/2} a_\mathrm{B} \qquad (\nu = 0) \tag{16}$$

$$l_{z0} \approx (1.6\ \mathrm{Ryd}/E^{(0)}) a_\mathrm{B} \qquad (\nu \geqslant 1). \tag{17}$$

Let us consider an atom moving along Oy. Both transverse sizes of the electron 'cloud' remain approximately independent of K: $l_x \approx l_y \approx l_{x0}$. However, the atom acquires a constant dipole moment $\boldsymbol{d} = e\langle \boldsymbol{r}_p - \boldsymbol{r}_e\rangle$ proportional to the mean proton–electron separation $\bar{x} = |\langle \boldsymbol{r}_e - \boldsymbol{r}_p\rangle|$. This separation is always smaller than r_c, and it approaches r_c at $K \gg K_\mathrm{c}$. With an accuracy of up to 10%, at $\gamma \geqslant 300$,

$$\bar{x}/r_\mathrm{c} \approx 1 - [1 + 0.015\gamma^2\sqrt{1+s}(E^{(0)})^{-4}]^{-1}[1 + (K/K_\mathrm{c})^{1/\alpha}]^{-1} - [1 + 0.004\gamma^2\,(E^{(2)}(K))^{-4}]^{-1}[1 + (K_\mathrm{c}/K)^{1/\alpha}]^{-1}, \tag{18}$$

where $E^{(0)}$, $E^{(2)}$, K_c and α are defined above.

The size of the electron cloud along the field is also affected by the motion. It can be

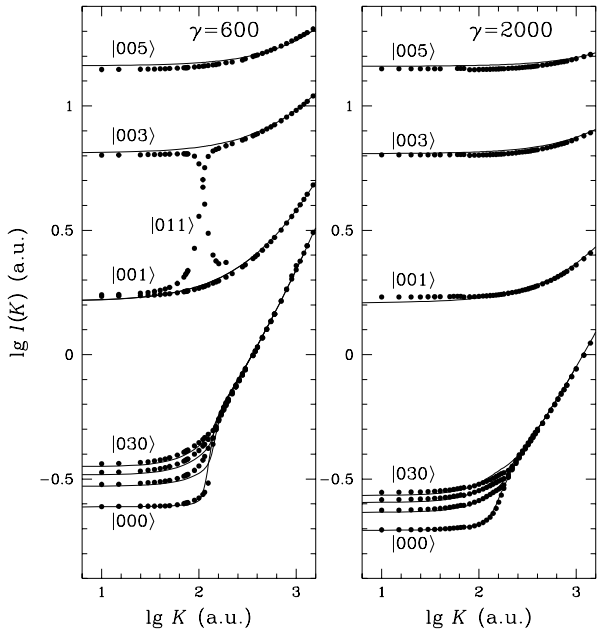

Figure 2. Comparison of calculated geometrical sizes of the atom (●) with the analytical approximations of section 4.1 (——).

described by the formulae

$$l_z = l_{z0}\frac{[1+(1-m_{\rm H}/m_{\rm eff})(K/K_{\rm c})^2]^{1/2}}{1+(K/K_{\rm c})^{1/\alpha}} + \frac{l_{z2}}{1+(K_{\rm c}/K)^{1/\alpha}} \qquad (\nu = 0) \tag{19}$$

$$l_z = (l_{z0}^2 + l_{z2}^2)^{1/2} \qquad (\nu \geqslant 1). \tag{20}$$

Here, l_{z0} is the value at $K = 0$ given by (16), (17), and

$$l_{z2} = \sqrt{\nu + \tfrac{1}{2}}[r_*^3 + (4.3 + 7\nu^2)r_*^2]^{1/4}$$

has the correct asymptotics at $K \to \infty$ (paper I).

In figure 2 the average size of the atom, $l(K) = [\bar{x}^2 + l_x^2 + l_y^2 + l_z^2]^{1/2}$, expressed through the above formulae, is compared with values calculated numerically. On the left panel (at $\gamma = 600$), the strong deviations of the numerical values from the fit for the states $|003\rangle$ and $|011\rangle$ at $K \sim 10^2$ au are caused by their anticrossing, which occurs shortly before the level (011) enters continuum. At $\gamma = 2000$ (right panel), this level belongs to the continuum at arbitrarily small K, so it does not (anti)cross truly bound levels.

4.2. Oscillator strengths

In this section we consider those oscillator strengths f that dominate photoabsorption of polarized radiation by ground-state hydrogen atoms at large γ. The polarization is assumed circular (right, for which we will use superscript '+', or left, '−') or linear, longitudinal ('‖') with respect to the static magnetic field.

At $K = 0$, the left-polarized radiation cannot excite the ground-state atom ($f^- = 0$), while right and longitudinally polarized radiation is absorbed mainly via transitions to the states $|010\rangle$ and $|001\rangle$, respectively. The corresponding oscillator strengths have been

computed and tabulated by Forster *et al* (1984). With an accuracy of 1–2%, at $0 \leqslant \gamma \leqslant 10^4$, they are reproduced by a single five-parameter formula

$$f^{\alpha}_{nsv}(0) = \left(1 - \frac{0.584}{1 + u_1\gamma^{u_2}}\right) \frac{1 + u_3\gamma}{1 + u_4\gamma^{u_5}}. \tag{21}$$

For $f^{+}_{010}(0)$, the parameteres u_i take on the values $u_1 = 12$, $u_2 = 1.43$, $u_3 = 9.8 \times 10^{-5}$, $u_4 = 1.585$ and $u_5 = 0.713$. For $f^{\parallel}_{001}(0)$, we have $u_1 = 2.64$, $u_2 = 1.076$, $u_3 = 6 \times 10^{-6}$, $u_4 = 0.247$ and $u_5 = 0.381$.

For the moving atom, in the restricted range $300 \leqslant \gamma \leqslant 10^4$, we put

$$f^{+}_{010}(K) = f^{+}_{010}(0) \frac{1 - a(K/K_{\rm c})^b}{1 + (K/K_{\rm c})^{1/\alpha'}} + \frac{2(m_{\rm e}/m_{\rm p})}{1 + (K_{\rm c}/K)^{1/\alpha'}}, \tag{22}$$

with $a = 1.28 - 0.267\ln(1+\gamma/240)$, $b = 1 + 3/[1 + \ln^2(1+\gamma/90)]$, $\alpha' = 0.012[1 + \ln^2(1 + \gamma/90)]$ and

$$f^{\parallel}_{001}(K) = f^{\parallel}_{001}(0)\exp[-(a'K/K_{\rm c})^2] + \frac{\exp[-(b'K/K_{\rm c})^{-\beta}]}{1 + 0.5\sqrt{K_{\rm c}/K}}, \tag{23}$$

with $a' = 0.877\ln(13100/\gamma)$, $b' = 0.89 - \gamma/17000$ and $\beta = 0.61\,(1 + 2410/\gamma)^{3/2}$. The second parts of (22) and (23) ensure the correct large-K limits ($2m_{\rm e}/m_{\rm p}$ and 1 respectively, cf paper I).

The radiative transitions forbidden for the atom at rest because of the conservation of the angular-momentum projection become allowed for the moving atom. In particular, the moving ground-state atom can absorb left-polarized radiaton. Oscillator strengths of such transitions are significant only at K of the order of $K_{\rm c} \sim 10^2$ au. Therefore we derive for them fitting formulae accurate to $\sim 10\%$ in this range of K and do not attempt to fit the complicated behaviour they show outside this range, where they are orders of magnitude smaller (paper I).

The transition to a state $|0s0\rangle$ presents the dominating absorption channel for circular polarization in a spectral range $E^{(0)}_{000} - E^{(0)}_{0,s-1,0} < \hbar\omega < E^{(0)}_{000} - E^{(0)}_{0s0}$ (where $\hbar\omega$ is a photon energy). For the right polarization, we put

$$f^{+}_{0s0}(K) = \frac{0.012(K/K_{\rm c})^{2s}(1 - K/K_{\rm c})}{1 + 11\ln(1 + (\gamma/3300)^2)} \qquad \text{at } K < K_{\rm c},\ s \geqslant 2, \tag{24}$$

and zero at $K \geqslant K_{\rm c}$; for the left polarization,

$$f^{-}_{0s0}(K) = \frac{1.3 \times 10^{-4}(K/K_{\rm c})^{2(s+1)}}{2^s[1 + (K/K_{\rm c})^{5(s+1)}]} \qquad (s \geqslant 1). \tag{25}$$

Although approximations (22)–(25) are rather crude, particularly owing to the anticrossings, their accuracy may still be sufficient for astrophysical applications, as will be demonstrated in the next section.

5. Spectral line shapes

As an application of the above fitting formulae, let us consider bound–bound absorption spectrum of hydrogen under the conditions typical for neutron-star atmospheres (Pavlov *et al* 1995): density $\rho \gtrsim 10^{-2}$ g cm^{-3}, temperature $T \sim 10^5$–10^6 K and magnetic field strength $B \sim 10^{12}$–10^{13} G. Such absorption spectra have been studied in paper II. Neglecting the Doppler and collisional broadening but taking into account the most important, magnetic broadening, one obtains an average partial cross section of an atom with respect to absorption

of polarized radiation with frequency ω via some specific transition $|\kappa\rangle \to |\kappa'\rangle$ as the sum $\sigma(\omega) = \sum_i \sigma_i(\omega)$ over the roots $K_i(\omega)$ of the equation $E'(K) - E(K) = \hbar\omega$, where $E'(K)$ ($E(K)$) is the energy of the final (initial) state of the atom, and

$$\sigma_i(\omega) = C_w^{-1} \frac{4\pi^3 e^2}{m_e c} K_i |\mathrm{d}K_i/\mathrm{d}\omega| w'(K_i) \exp[-E(K_i)/k_B T] f(K_i). \tag{26}$$

Here, $f(K)$ is the oscillator strength for the given transition and polarization, k_B is the Boltzmann constant,

$$C_w = 2\pi \int_0^\infty K w(K) \exp[-E(K)/k_B T] \, \mathrm{d}K \tag{27}$$

is a normalization constant and $w'(K)$ ($w(K)$) is the occupation probability of the final (initial) atomic state in a plasma with a number density of electrons n_e. These occupation probabilities can be estimated as $w \sim \exp[-(4\pi/3) n_e (4l)^3]$, where l is the rms radius of the atom. This expression is pertinent to the calculation of the bound–bound absorption considered here. To calculate the thermodynamic properties of the plasma, however, one should use, instead of these 'optical' occupation probabilities, 'thermodynamical' ones, which are generally larger (Potekhin 1996).

In order to take into account induced emission, $\sigma_i(\omega)$ should be multiplied by $(1 - \mathrm{e}^{-\hbar\omega/k_B T})$. The collisional broadening can be taken into account by convolution of $\sigma_i(\omega)$ with the Lorentzian profile characterized by the width $\Gamma(K_i(\omega))$ (paper II). Since this type of broadening has only marginal significance compared with the magnetic broadening in the neutron-star atmospheres, we employ a simple order-of-magnitude estimate:

$$\Gamma(K) \approx \Gamma_0 n_e a_B^3 (k_B T/\mathrm{Ryd})^{1/6} (1 + 2r_*^{5/6}), \tag{28}$$

where $\Gamma_0 \approx 15$ au for transitions to the state $|001\rangle$ (that mainly determine absorption of radiation polarized longitudinally) and $\Gamma_0 \approx (68/\gamma)$ au for transitions to the state $|010\rangle$ (responsible for the main absorption peak of circular polarization).

Some of the typical absorption profiles obtained numerically in paper II are represented by full lines in figure 3. The spectral range is shown that is relevant to interpretation of spectral observations of neutron stars with the x-ray telescope on-board ROSAT satellite (e.g. Pavlov *et al* 1995). Approximate profiles, obtained using the analytical approximations of section 3.2 for $E(K)$, the formulae of section 4 for $l(K)$ and $f(K)$ and the estimate (28) for $\Gamma(K)$, are shown in figure 3 by broken curves. One can see that they correctly reproduce the gross features of the spectral shapes, thus the proposed approximations are suitable for using them in theoretical models of neutron-star atmospheres compatible with contemporary observational data. The figure demonstrates also the importance of the decentred states: for example, the absorption of longitudinally polarized radiation at $\hbar\omega < 100$ eV is produced solely by the states of motion with $K > K_c$.

In reality, observed spectra are influenced not only by the bound-bound photoabsorption shown in figure 3 but also by bound–free transitions. For moving atoms, bound–free cross sections were calculated by Potekhin and Pavlov (1997). Under conditions typical of atmospheres of cooling neutron stars, maximum bound–free photoabsorption turns out to be of the same order of magnitude as the bound–bound one, but it is shifted to higher-photon energies. In the spectral range shown in figure 3, the bound–free transitions are generally less important.

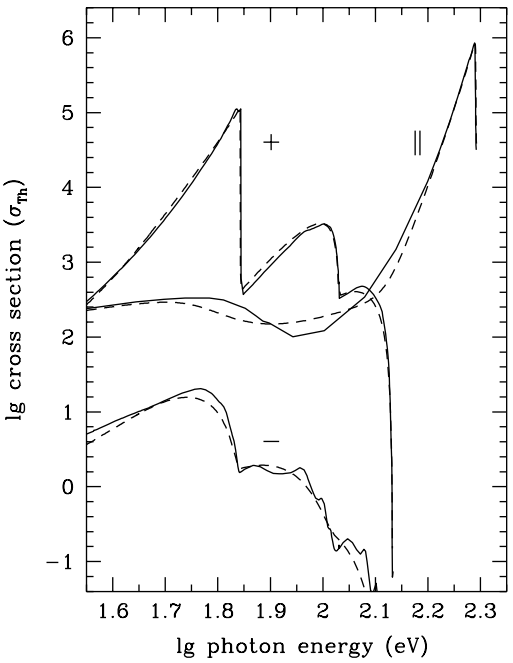

Figure 3. Comparison of numerically calculated (——) and approximate (– – –) spectral shapes for bound–bound absorption of right (+), left (−) and longitudinally (‖) polarized radiation by hydrogen atoms in thermal equilibrium with plasma under the conditions typical for atmospheres of magnetic neutron stars: $k_{\rm B}T = 1$ Ryd ($T = 1.58 \times 10^5$ K), $\rho = 0.01$ g cm^{-3}, and $\gamma = 10^3$ ($B = 2.35 \times 10^{12}$ G).

6. Conclusions

We have obtained analytical approximations of binding energies, geometrical sizes and main oscillator strengths of radiative transitions of the hydrogen atom moving across a strong magnetic field. These approximations can be also applied to the hydrogen atom in crossed electric and magnetic fields, since the latter problem reduces to the former one with the effective pseudomomentum $K = m_{\rm H}c\mathcal{E}/\mathcal{E}_c$, or equivalently K (au) $= 8.4(\mathcal{E}/\text{V m}^{-1})(B/\text{G})^{-1}$.

Binding energies are the most important quantities in many applications and for that reason we have presented not only fitting formulae depending analytically on γ and K (section 3.2), but also considerably more accurate K-dependences at six selected values of γ (section 3.1). Atomic sizes (section 4.1) play an important role in the distribution of atoms over quantum states in a plasma and in their contribution to the plasma absorption coefficients. For example, the size of an atom may be used to evaluate effects of 'unbinding' of electrons caused by random charge distribution in the plasma. For non-magnetized hydrogen plasmas, an approximate treatment of these effects was revised recently (Potekhin 1996); for strong magnetic fields analogous work is under way. The approximations of oscillator strengths (section 4.2), along with those of the energies and sizes, facilitate calculations of absorption spectra of strongly magnetized, partially ionized hydrogen plasmas. Eventually, the analytical estimates of γ- and K-dependences of the binding energies, atomic sizes and transition rates will help to generalize previously developed models of fully ionized atmospheres of magnetic neutron stars (Shibanov *et al* 1992) to the more realistic case of partially ionized atmospheres.

Acknowledgments

This work was inspired by stimulating discussions with participants of the 172 WE-Heraeus-Seminar on Atoms and Molecules in Strong External Fields (Bad Honnef, 7–11 April 1997) organized by Dr Peter Schmelcher and Dr Wolfgang Schweizer. I wish to express my gratitude to Professor Joachim Trümper and Dr Vyacheslav Zavlin for hospitality during my visit at the Max-Planck-Institut für Extraterrestrische Physik in Garching, where a large part of this work has been performed using the MPE computing facilities. The visit was made possible due to the DFG–RFBR grant no 96-02-00177G. Partial support from the RFBR grant no 96-02-16870a and INTAS grant no 94-3834 is also acknowledged. I am grateful to Professor Joseph Ventura for useful discussions and hospitality at the University of Crete, where the final part of this work was completed.

References

Avron J E, Herbst I W and Simon B 1978 *Ann. Phys., NY* **114** 431–51
Baye D, Clerbaux N and Vincke M 1992 *Phys. Lett.* A **166** 135–9
Baye D and Vincke M 1990 *Phys. Rev.* A **42** 391–6
Braun P A and Solov'ev E A 1984 *J. Phys. B: At. Mol. Phys.* **17** L211–16
Burkova L A, Dzyaloshinskii I E, Drukarev G P and Monozon B S 1976 *Sov. Phys.–JETP* **44** 276–8
Chen Z and Goldman S P 1992 *Phys. Rev.* A **45** 1722–31
Dippel O, Schmelcher P and Cederbaum L S 1994 *Phys. Rev.* A **49** 4415–29
Dzyaloshinskii I E 1992 *Phys. Lett.* A **165** 69–71
Elliott R J and Loudon R 1960 *J. Phys. Chem. Solids* **15** 196–207
Fassbinder P and Schweizer W 1996 *Astron. Astrophys.* **314** 700–6
Forster H, Strupat W, Rösner W, Wunner G, Ruder H and Herold H 1984 *J. Phys. B: At. Mol. Phys.* **17** 1301–19
Gorkov L P and Dzyaloshinskii I E 1968 *Sov. Phys.–JETP* **26** 449–58
Haines L K and Roberts D H 1969 *Am. J. Phys.* **37** 1145–54
Ipatova I P, Maslov A Y and Subashiev A V 1984 *Sov. Phys.–JETP* **60** 1037–9
Ivanov M V 1988 *J. Phys. B: At. Mol. Opt. Phys.* **21** 447–62
Johnson B R, Hirschfelder J O and Yang K-H 1983 *Rev. Mod. Phys.* **55** 109–53
Lai D and Salpeter E E 1995 *Phys. Rev.* A **52** 2611–23
Klaassen T O, Dunn J L and Bates C A 1997 *Proc. 172 WE-Heraeus-Seminar 'Atoms and Molecules in Strong External Fields' (Bad Honnef, 7–11 April)* ed P Schmelcher and W Schweizer (New York: Plenum) in press
Kravchenko Yu P, Liberman M A and Johansson B 1996 *Phys. Rev.* A **54** 287–305
Melezhik V S 1993 *Phys. Rev.* A **48** 4528–38
Pavlov G G and Mészáros P 1993 *Astrophys. J.* **416** 752–61
Pavlov G G and Potekhin A Y 1995 *Astrophys. J.* **450** 883–95 (paper II)
Pavlov G G, Shibanov Yu A, Zavlin V E and Meyer R D 1995 *The Lives of the Neutron Stars (Proc. NATO ASI C 450)* ed M A Alpar, Ü Kiziloğlu and J van Paradijs (Dordrecht: Kluwer) pp 71–90
Potekhin A Y 1994 *J. Phys. B: At. Mol. Opt. Phys.* **27** 1073–90 (paper I)
——1996 *Phys. Plasmas* **3** 4156–65
Potekhin A Y and Pavlov G G 1993 *Astrophys. J.* **407** 330–41
——1997 *Astrophys. J.* **483** 414–25
Rösner W, Wunner F, Herold H and Ruder H 1984 *J. Phys. B: At. Mol. Phys.* **17** 29–52
Ruder H, Wunner G, Herold H and Geyer F 1994 *Atoms in Strong Magnetic Fields* (Berlin: Springer)
Schmelcher P 1993 *Phys. Rev.* B **48** 14 642–5
Shibanov Yu A, Zavlin V E, Pavlov G G and Ventura J 1992 *Astron. Astrophys.* **266** 313–20
Taylor J H, Manchester R N and Lyne A G 1993 *Astrophys. J. Suppl. Ser.* **88** 529–68
Vincke M and Baye D 1988 *J. Phys. B: At. Mol. Opt. Phys.* **21** 2407–24
Vincke M, Le Dourneuf M and Baye D 1992 *J. Phys. B: At. Mol. Opt. Phys.* **25** 2787–807
Wintgen D and Friedrich H 1986 *J. Phys. B: At. Mol. Phys.* **19** 991–1011
Wunner G and Ruder H 1987 *Phys. Scr.* **36** 291–9
Xi J, Wu L, He X and Li B 1992 *Phys. Rev.* A **46** 5806–11